UC San Diego
UC San Diego Previously Published Works

Title

Continuity and Discontinuity in Human Cortical Development and Change From Embryonic Stages to Old Age.

Permalink

https://escholarship.org/uc/item/4021m9kf

Journal

Cerebral Cortex, 29(9)

ISSN

1047-3211

Authors

Fjell, Anders M
Chen, Chi-Hua
Sederevicius, Donatas
et al.

Publication Date

2019-08-14

DOI

10.1093/cercor/bhy266

Peer reviewed

OXFORD

ORIGINAL ARTICLE

Continuity and Discontinuity in Human Cortical Development and Change From Embryonic Stages to Old Age

Anders M. Fjell [1,2], Chi-Hua Chen[3], Donatas Sederevicius[1],
Markus H. Sneve [1], Håkon Grydeland [1], Stine K. Krogsrud[1],
Inge Amlien[1], Lia Ferschmann[1], Hedda Ness[1], Line Folvik[1], Dani Beck[1],
Athanasia M. Mowinckel[1], Christian K. Tamnes[1], René Westerhausen[1],
Asta K. Håberg[4,5], Anders M. Dale[3,6] and Kristine B. Walhovd[1,2]

[1]Department of Psychology, Center for Lifespan Changes in Brain and Cognition, University of Oslo, 0317 Oslo,
Norway, [2]Department of Radiology and Nuclear Medicine, Oslo University Hospital, 0372 Oslo, Norway,
[3]Department of Radiology, University of California, San Diego, La Jolla, CA 92093, USA, [4]Department of Medical
Imaging, St. Olav's Hospital, 7491 Trondheim, Norway, [5]Department of Neuroscience, Norwegian University of
Science and Technology (NTNU), N-7491 Trondheim, Norway and [6]Department of Neurosciences, University of
California, San Diego, La Jolla, CA 92093, USA

Address correspondence to Anders M. Fjell, Department of Psychology, Center for Lifespan Changes in Brain and Cognition, University of Oslo, Pb. 1094
Blindern, 0317 Oslo, Norway. Email: andersmf@psykologi.uio.no orcid.org/0000-0003-2502-8774

Abstract

The human cerebral cortex is highly regionalized, and this feature emerges from morphometric gradients in the cerebral
vesicles during embryonic development. We tested if this principle of regionalization could be traced from the embryonic
development to the human life span. Data-driven fuzzy clustering was used to identify regions of coordinated longitudinal
development of cortical surface area (SA) and thickness (CT) ($n = 301$, 4–12 years). The principal divide for the developmental
SA clusters extended from the inferior–posterior to the superior–anterior cortex, corresponding to the major embryonic
morphometric anterior–posterior (AP) gradient. Embryonic factors showing a clear AP gradient were identified, and we
found significant differences in gene expression of these factors between the anterior and posterior clusters. Further, each
identified developmental SA and CT clusters showed distinguishable life span trajectories in a larger longitudinal dataset
(4–88 years, 1633 observations), and the SA and CT clusters showed differential relationships to cognitive functions. This
means that regions that developed together in childhood also changed together throughout life, demonstrating continuity
in regionalization of cortical changes. The AP divide in SA development also characterized genetic patterning obtained in an
adult twin sample. In conclusion, the development of cortical regionalization is a continuous process from the embryonic
stage throughout life.

Key words: aging, cognition, cortical development, magnetic resonance imaging, protomap theory

Expansion of cortical surface area (SA) in human development is highly regionalized (Amlien et al. 2016). According to the protomap (Rakic 1988) and radial unit models (Rakic et al. 2009), the blueprint for this regional cortical expansion is established already in early embryonic development. Cortical neurons are not born within the cerebral cortex itself but migrate from the ventricular zone to their final destination. The major morphometric gradient governing areal identity runs along the anterior–posterior (AP) axis (Rakic et al. 2009). However, it is not known if the governing principles of embryonic brain development apply to cortical expansion in children. In the present study, we tested this hypothesis, which would show a continuity of cortical expansion from the early fetal to the latest stages of development in the pre-teen years.

Moreover, the related tenet that late-life brain health and cognitive function have developmental origins is getting increasing support (Jagust 2016; Walhovd et al. 2016). Adult genetic SA topography—the delineation of regions influenced by the same genes—is characterized by an AP gradient, likely due to prenatal factors (Rakic 2009; Walhovd et al. 2012), corresponding to our hypothesis for organization of SA development. Thus, an intriguing possibility is that the fundamental organizational principles for regional brain development in children, likely reflecting patterns from embryonic development, can be traceable also in higher age. This would mean that anatomical regions that develop together also show distinct life span trajectories of adult cortical change and decline in aging. We know that cortical maturation to some degree proceeds along functional and structural networks established in adults (Zielinski et al. 2010; Raznahan, Lerch, et al. 2011; Alexander-Bloch et al. 2013; Walhovd et al. 2015; Krongold et al. 2017; Sotiras et al. 2017), but not whether brain regions that develop together also change together through the rest of life. Testing this was the second main aim of the project.

These hypotheses were addressed through several steps. First, a data-driven fuzzy clustering approach was used to parcellate longitudinal change in SA and apparent thickness (CT) of the cerebral cortex into regions of coordinated development. CT and SA develop differently (Raznahan, Shaw, et al. 2011; Amlien et al. 2016; Walhovd et al. 2017) and have different genetic and molecular foundations (Rakic 1988; Panizzon et al. 2009; Rakic et al. 2009). We selected an age range when SA still expands and apparent CT is continuously declining, that is, 4–12 years (n = 301). Clustering was based on 1.5 years of longitudinal change to avoid confounds from cross-sectional differences. The principal axes of the developmental clusters were extracted and tested against the AP morphometric gradient from gene expression patterns in embryonic development, identified by Rakic et al. (2009).

The developmental clusters were further tested against genetic cortical topography established in an adult sample of twins (Chen et al. 2012, 2013). CT shows more age change and is more affected by later-life events than SA (Engvig et al. 2010; Wenger et al. 2012; Storsve et al. 2014), and the original genetic patterning work predicted that CT clusters, more than SA clusters, would show genetic relatedness with clusters of similar maturational timing (Chen et al. 2013). Thus, we hypothesized that developmental SA change would adhere more closely to prenatal gene expression gradients, while CT change clusters would be more similar to genetic clusters obtained from adult twins (Fjell et al. 2015).

Next, we tested if the developmental clusters showed different age trajectories in a longitudinal dataset covering more than 8 decades (4.1–88.5 years, n = 974, 1633 scans). On the

assumption of continuity between fetal and child development and lasting impacts of early-life factors on later brain changes, we hypothesized that the residual variance in each developmental cluster would be differentially related to age when the common variance shared among the clusters was accounted for. This means that we expected each developmental cluster to show different life span trajectories.

Finally, we tested whether the developmental clusters showed differential relationships to 4 empirically derived domains of cognitive function—episodic memory, executive speed, working memory, and general cognitive ability (GCA). These domains were identified from a principal component analysis (PCA) of multiple cognitive scores from an extended longitudinal dataset (4.1–93.4 years, 4065 observation). As SA and CT have different early determinants and show different developmental and life span trajectories, we hypothesized different relationships to cognition. We expected the SA clusters to relate to GCA, which is likely heavily influenced by early-life factors and shows high life span stability (Lyons et al. 2009; Deary et al. 2012; Vuoksimaa et al. 2015; Walhovd et al. 2016). The scores included in the GCA component (matrix reasoning and vocabulary) load strongly on the g-factor (Deary et al. 2010) and have previously been found to correlate more with SA than CT (Vuoksimaa et al. 2015; Walhovd et al. 2016). As likely more amendable to environmental influences through life, CT was hypothesized to correlate more strongly with more specific cognitive functions, indicated by lower loadings on the g-factor. These could include episodic memory and executive speed, which show different change trajectories across people (Salthouse 2016) and are less strongly related to global cognitive change (Tucker-Drob 2011).

Materials and Methods

Sample

A total of 1633 valid scans from 974 healthy participants (508 females/466 males), 4.1–88.5 years (mean visit age 25.8, SD 24.1), were drawn from 3 Norwegian studies coordinated by the Research Group for Lifespan Changes in Brain and Cognition; The Norwegian Mother and Child Cohort Neurocognitive Study (MoBa)/Neurocognitive Development (ND)/Cognition and Plasticity Through the Lifespan (CPLS) (see Supplementary Material for details). 635 participants had 2 scans and 24 had 3 (mean scan interval 2.3 years [0.2–6.6]). The sample is identical to Fjell et al.'s (2015). All were screened for conditions assumed to affect CNS function. Number of observations in different age spans is provided in Table 1.

The cluster-forming sample consisted of all MoBa participants with 2 scans (n = 301, 602 scans in total, mean age 7.3 years [range 4.1–12.0], mean scan interval 1.5 years [1.0–2.2]). This is a population-based sample, with participants recruited by the Norwegian Medical Birth Registry through the national Norwegian Mother and Child Cohort Study (82), see (8, 83) and

Table 1 Number of observations

	Obs	n	Age[a]	Follow-up interval
<20 years	1021	644	9.2 (4.1–19.7)	1.7 (1.0–3.2)
20–50 years	234	136	35.2 (20–50)	3.2 (0.2–6.3)
>50 years	378	194	64.8 (50.5–85.3)	1.6 (0.2–6.6)

[a]Age at baseline.
Note: Obs, number of observations; n, number of participants.

Supplementary Material for details. The age range is well covered, with good sample density across.

The twin sample used to generate the genetic clusters consisted of 406 middle-aged men (55.8 years [51–59]), including 110 monozygotic and 93 dizygotic twin pairs, from the Vietnam Twin Study of Aging (see Supplementary Material and (Kremen et al. 2013) for details).

Cognitive Testing

All participants underwent extensive neuropsychological testing. Cognitive test scores were entered into a PCA with varimax rotation with Kaiser normalization. The following test scores were included in the analysis: verbal learning (California Verbal Learning Test [CVLT], sum of trials 1–5), 30-min recall and 30-min recognition (Delis et al. 2000), Stroop reading, Stroop color naming and Stroop incongruent color naming (MacLeod 1992), digit span forward and backward (Wechsler 2008), vocabulary and matrix reasoning (Wechsler 1999), see Supplementary Material for details about the tests. In contrast to the measured scores, the PCA-derived components are free of measurement errors. To obtain a stable and generalizable component solution, the PCA was run on a larger healthy sample from the same research center, screened with the same instruments as the MRI subsample, containing 4065 participant observations (age 4.1–93.4 years, 2285/1722 females/males observations), inclusive of those used in the present study. In the case of missing values, the "mean substitution" method was used. Inspection of the scree plot revealed that both 3 and 4 components were reasonable solutions. The 4-component solution gave most sense from a neuropsychological perspective, and the 4-component solution was thus chosen for further analyses, yielding 81.53% explained variance. See Table 2 and Supplementary Material for details.

To ensure that the PCA from the larger samples was representative also for the subsample used in the present paper, Procrustes rotation was used to assess the degree of dissimilarity. This procedure rotates a matrix to maximum similarity with a target matrix minimizing the sum of squared differences. 10.000 permutations were run, yielding a P-value of $9.999e^{-05}$, sum of squares of 0.099, and a correlation for a symmetric Procrustes rotation of 0.95, indicating excellent correspondence between the matrices. This was further confirmed by a Mantel permutation test for similarity of 2 matrices,

Table 2 Rotated component matrix

	Memory	Executive speed	Working memory	GCA
Recall 30 min	0.86			
Learning	0.82			
Recognition	0.81			
Stroop words		0.92		
Stroop colors		0.85		
Stroop colors/ words		0.83		
Digit span forward			0.87	
Digit span backward			0.78	
Vocabulary				0.82
Matrix reasoning	0.47			0.69

Note: Values below 0.40 are suppressed. Rotation method: varimax with Kaiser normalization. Rotation converged in 5 iterations. GCA, general cognitive ability. Recall, learning and recognition from CVLT, vocabulary and matrix from WASI.

yielding an observed r of 0.95 and a simulated P-value of $9.999e^{-05}$ for 10.000 permutations. Thus, applying the PCA solution from the larger sample to the MRI subsample was clearly a valid approach.

MRI Data Acquisition and Analysis

Imaging data (except VETSA) were acquired using a 12-channel head coil on 2 1.5-Tesla Siemens Avanto scanners (Siemens Medical Solutions, Erlangen, Germany), yielding 2 repeated 3D T1-weighted magnetization prepared rapid gradient echo (MPRAGE): TR/TE/TI = 2400 ms/3.61 ms/1000 ms, FA = 8°, acquisition matrix 192 × 192, FOV = 240 mm, 160 sagittal slices with voxel sizes 1.25 × 1.25 × 1.2 mm. For most children 4–9 years old, integrated parallel imaging (iPAT) was used, acquiring multiple T1 scans within a short scan time with the same parameters as above, enabling us to discard scans with residual movement and average the scans with sufficient quality. Previous studies have shown that accelerated imaging does not introduce significant measurement bias in surface-based measures when using FreeSurfer for image analysis, compared with a standard MPRAGE protocol with otherwise identical voxel dimensions and sequence parameters (97), which is in accordance with our own analyses.

MRI data (except VETSA) were processed and analyzed with FreeSurfer 5.3 (http://surfer.nmr.mgh.harvard.edu/) (Dale and Sereno 1993; Dale et al. 1999) longitudinal stream (Fischl and Dale 2000; Reuter and Fischl 2011; Reuter et al. 2012). SA maps were smoothed using a circularly symmetric Gaussian kernel with a full width at half maximum (FWHM) of 26 mm and CT maps with a kernel of 21 FWHM. Movement is a major concern (Reuter et al. 2015), so scans were manually rated 1–4, and only 1 or 2 (no visible or only very minor possible signs of movement) were included. Also, all reconstructed surfaces were inspected and discarded if they did not pass internal quality control. This led to the exclusion of 46 participants from MoBa-Neurocog and 9 from ND, reducing the total sample to the reported 1633 scans.

For VETSA, images were acquired on 2 Siemens 1.5-Tesla scanners. Sagittal T1-weighted MPRAGE sequences were employed with a TI = 1000 ms, TE = 3.31 ms, TR = 2730 ms, flip angle = 7°, slice thickness = 1.33 mm, voxel size 1.3 × 1.0 × 1.3 mm. Similar to the other data, the scans were run through FreeSurfer and manually inspected and quality checked, with minimal manual editing performed. Details about the VETSA MRI processing can be found here (Chen et al. 2013).

Fuzzy Clustering

The fuzzy clustering procedure was performed using the "cluster" package implemented in R (www.r-project.org/). The individual de-meaned annualized symmetrized percentage change (APC) maps were fed into the cluster algorithm. The APC maps were computed by calculating the difference in thickness/area for each vertex between timepoints, divide by the mean thickness/area across timepoints for that vertex, and multiply by 100. Clustering methods partition the dataset into clusters based on the chosen proximity relations. We calculated pairwise correlations of thickness and area change between every 2 vertices on the cortex for the left and right hemispheres separately. To reduce computation time, we subsampled the standardized cortical surface tessellation from the original 163.842–2.562 vertices per hemisphere. We then transformed the change correlation matrix into the distance matrix by

subtracting each correlation from 1. In fuzzy clustering, objects can belong to more than one cluster and with different degrees of membership to the different clusters, between 0 and 1. Thus, the memberships of objects at the overlapping boundaries will typically express the ambiguity of the cluster assignment. Fuzzy clustering aims to minimize the objective function

$$\sum_{v=1}^{k} \frac{\sum_{i=1}^{n} \sum_{j=1}^{n} u_{iv}^{r} u_{jv}^{r} d(i, j)}{2 \sum_{j=1}^{n} u_{jv}^{r}},$$

where n is the number of observations, k is the number of clusters, r is the membership exponent, u is the cluster membership, and $d(i, j)$ is the dissimilarity between observations i and j (Kaufman and Rousseeuw 1990). The cluster memberships u are non-negative and sum to one for a given data point. To investigate the stability of the clustering in relation to initialization, we randomly initialized the algorithm for 100 runs and picked the cluster solution that maximized the likelihood function.

In addition, we generated random clusters to compare with the power of the real clusters. The performance of the developmental clusters was compared with randomly generated clusters for a 3-cluster solution, since the 3-cluster solution was used for the life span analyses (see the following). The random clusters were generated using k-means algorithm implemented in MATLAB (R2015b). The spatial locations of the cerebral cortex mesh were partitioned into 15 clusters using the squared Euclidean distance metric and k-means++ algorithm for cluster center initialization. One of the clusters resulted in capturing the whole temporal lobe, therefore, it was further subdivided into 4 clusters using the same procedure. The final 18 clusters were merged into 3 clusters of similar size to the empirically derived clusters.

Genetic Clustering

The developmental clusters were compared with previously published genetic clusters (Chen et al. 2013), made accessible for formal comparisons to the present study. The genetic clusters were derived using a similar Fuzzy clustering approach to the one described above. The clustering was performed on genetic correlation maps for cortical thickness and area based on the VETSA sample. The resulting clusters represent boundaries of cortical divisions that are maximally under control of shared genetic influences. The present 2- and 3-cluster solutions for cortical thickness and area development were compared with the genetic 2- and 3-cluster thickness and area solutions by use of the Rand Index (see the following).

Gene Expression Analyses

Cortical gene expression data were obtained from the BrainSpan Atlas of the Developing Human Brain (2010) (www.brainspan.org) (Miller et al. 2014), which provides a transcriptome of the developing human brain. We rated 31 transcription factors assumed responsible for shaping the partitioned neocortex (Rakic et al. 2009) according to how well their expression patterns were aligned to the AP axis. 18 factors showed a clear and 4 a partial AP gradient, yielding evidence that the AP axis constitutes a major regionalization gradient in early cortical development. To test whether this cluster gradient could be detected in later human gene expression patterns, we selected the candidate with the most established AP expression pattern, *PAX6* (Bishop et al. 2000), and the candidate with the most

pronounced AP expression pattern, P75 (Rakic et al. 2009). Thirty-four out of the 42 donor brains in the BrainSpan Atlas had valid probe data from at least one cortical region within each of the empirically derived developmental clusters (see the following). Mean expression values for cortical regions falling within the developmental clusters were extracted for the 34 participants from the BrainSpan Atlas. For each donor, the average *PAX6/P75* expression was estimated through mean averaging of normalized expression values (Reads Per Kilobyte Million; RPKM) from cortical samples overlapping with the developmental clusters.

Statistical Analyses

Analyses were run in R (https://www.r-project.org) using Rstudio (www.rstudio.com) IDE, except the PCA (SPSS v25). The Rand index (RI) and Silhouette plots (Rand 1971), in combination with visual inspections, were used to inform the choice of specific cluster solutions. RI is a number between 0 and 1 that quantifies the degree of similarity between 2-cluster solutions by computing the proportion of vertices that are given the same cluster label in both solutions. It is possible for some vertices to have the same cluster label by chance, and this is accounted for in the adjusted RI. Adjusted RI was used to compare area with thickness clusters, and the developmental clusters to the genetic clusters.

To characterize each 2-cluster solution according to the main axes (AP, inferior–superior [IS], lateral-medial [LM]), the cortical surface was divided in 20 bins along each axis. The mean probability of all the vertices within each bin along the AP axis to belong to a given cluster was calculated, and the same for the IS and LM axes. These values were then correlated with the axis bin numbers (from 1 to 20), yielding an objective measure of how much of the variance of the different cluster solutions that could be explained by each of the 3 principal axes.

Generalized Additive Mixed Models (GAMMs) implemented in R (www.r-project.org) using the package "mgcv" (Wood 2006, 2011) were used to derive age functions for morphometric and cognitive variables. Akaike information criterion (AIC) (Akaike 1974) and the Bayesian information criterion (BIC) were used to guide model selection and help guard against overfitting. The smoothness of the age curve is estimated as a part of the model fit, and the resulting effective degree of freedom (edf) was taken as a measure of deviation from linearity. The P-values associated with the smooth terms are only approximate, as they are based on the assumption that a penalized fit is equal to an unpenalized fit with the same edf, and do not take into account uncertainty associated with the smoothing parameter estimation. The major advantage of GAMM in the present setting is that relationships of any degree of complexity can be modeled without specification of the basic shape of the relationship, and GAMM is thus especially well suited to map life span trajectories of neurocognitive variables which can be assumed to be nonlinear and where the basic form of the curve is not known (Fjell et al. 2010). Sex was used as a covariate in the area analyses, as sex is related to area but less to thickness (Fjell et al. 2009).

Results

Clusters of Cortical Change in Development of 4–12 Years

Clusters are presented in Fig. 1 (SA) and Fig. 2 (CT). The 2-cluster SA solution followed a clear AP (correlation with the
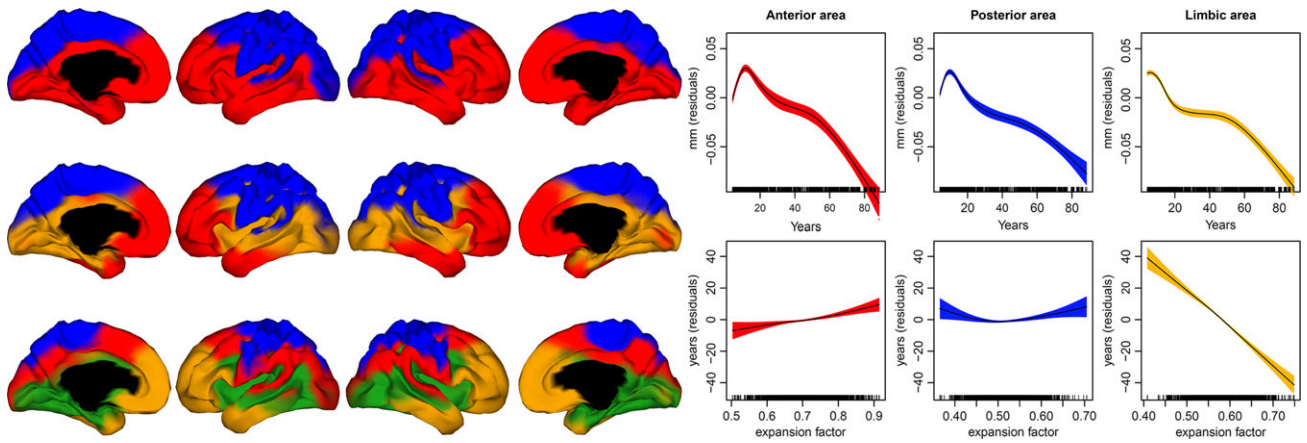
Figure 1. Surface area. Left panel: Clusters of coordinated SA in development, 2- (top), 3- (middle), and 4-cluster (bottom) solutions. Right panel: The life span trajectories of each cluster from the 3-cluster solution. Top: Trajectories residualized on age (x-axis). Bottom: The residual age relationship (y-axis) for each cluster accounting for the other 2 clusters. These curves show the relationship between each cluster and age, if the common variance shared with the other clusters are accounted for. Relative to the other clusters, the anterior cluster shows a slight increase with age (larger cluster area goes with older age), while the limbic cluster shows a linear decline (larger cluster area goes with younger age). The colors of the curves correspond to the cluster color in the left figure. The shaded area denotes ±2 standard errors of the mean.
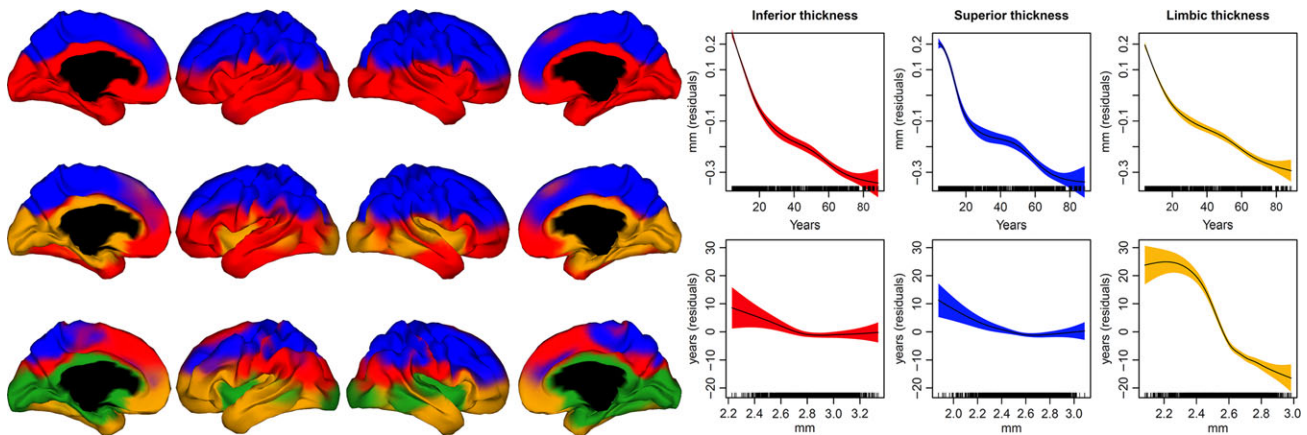

Figure 2. Cortical thickness. Left panel: Clusters of coordinated cortical thickness in development, 2- (top), 3- (middle), and 4-cluster (bottom) solutions. Right panel: The life span trajectories of each cluster from the 3-cluster solution. Top: Trajectories residualized on age (x-axis). Bottom: The residual age relationship (y-axis) for each cluster accounting for the other 2 clusters (see Fig. 1 legend for explanation). The colors of the curves correspond to the cluster color in the left figure. The shaded area denotes ±2 standard errors of the mean.

AP axis $r = 0.91$) and IS ($r = 0.97$) gradient, with less influence from the LM ($r = 0.19$) axis. The AP division was tilted 19° from the base plane, causing the strong IS correlation. The posterior cluster covered the central sulcus and the adjacent anterior regions of the frontal cortex (premotor cortex), extending back to encapsulate the dorsolateral occipital cortex, and inferiorly down to the cingulum. For the 3-cluster solution, an occipital-limbic cluster emerged. In the 4-cluster solution, a new cluster appeared inferior to the first posterior cluster, distinguishing this cluster from the rest of the clusters both medially and laterally.

The 2-cluster CT solution showed a very strong IS gradient ($r = 0.97$), with less AP (0.39) and LM (0.46) influence. With 3 clusters, an occipital-limbic cluster emerged. In the 4-cluster solution, the superior cluster was split in 2 clusters. For both CT and SA, the silhouette values flattened after 4 clusters, suggesting that 5 clusters were too many (see Supplementary Material). The adjusted Rand Index (adj RI) showed substantial overlap between the 2-cluster SA and CT solutions (adj RI = 0.88), with less similarity for 3 (adj RI = 0.27) and 4 (adj RI = 0.22) clusters. Still, the medial limbic cluster and the prefrontal–anterior–temporal relationship was similar between SA and for CT across the 3- and 4-cluster solutions.

To validate the Fuzzy clustering results, we ran seed point analyses from 360 seeds based on a multimodal parcellation scheme (Glasser et al. 2016). The critical features of the cluster results were confirmed, including the AP axis for SA, the IS axis for CT, and the prefrontal–temporal relationship and delineation of the limbic clusters for both SA and CT (see Supplementary Material).

Adherence of SA Development to Early Morphometric Gradients

Mean expression values for *PAX6/ P75* in cortical regions falling within the anterior and the posterior developmental clusters

were extracted for 34 participants from the BrainSpan Atlas (www.brainspan.org). Five samples from the atlas fell within the superior–anterior cluster: samples from dorsolateral prefrontal cortex, ventrolateral prefrontal cortex, orbital frontal cortex, inferolateral temporal cortex, and anterior cingulate cortex. Four samples fell within the inferior–posterior cluster: primary motor cortex, primary somatosensory cortex, posteroventral parietal cortex, and primary auditory cortex. Difference in expression between the superior–anterior cluster and the inferior–posterior cluster was assessed for PAX6 and P75(NGFR) separately using paired-samples t-tests. Expression values of

PAX6 were significantly higher (t = 4.24, df = 33, P < 0.0002) in the anterior than the posterior development cluster, while the opposite was found for P75 (t = −3.03, df = 33, P < 0.005) (Fig. 3). Put together, this shows that traces of the major expression patterns in embryonic development can be recovered in later childhood, and that the gene expression patterns in humans follow cortical change in ways predicted from early embryonic development. It was not given that genes with strong AP gradients during embryonic brain development would also adhere to an empirically derived AP cluster solution based on cortical changes during childhood development.
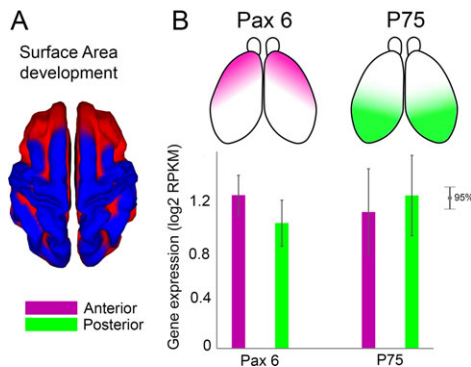
Resemblance to Cortical Genetic Patterning

After having established that SA development follows the main AP gradient identified in embryonic development, we tested how similar the developmental SA and CT clusters were to mid-life genetic cortical topography (Chen et al. 2013) (Fig. 4). Genetic topography represents the delineation of regions influenced by the same genes. RI suggested low overlap (adj RI < 0.10 for 2- and 3-cluster solutions) between genetic topography and the developmental clusters. The AP division was seen for both, but the boundary between the clusters was shifted from inferior–posterior to anterior–superior for the development clusters (−71° from the perpendicular axis) compared with inferior–anterior to superior–posterior (+38°) for the genetic clusters. Adherence to the AP axis was slightly higher for the genetic (r = 0.96) versus the developmental (r = 0.91) clusters, and slightly lower for the IS axis (r = 0.82 for genetics versus r = 0.91 for development).

Figure 3. Genetic patterns. (A) SA-developmental clusters, top view. (B) AP gradient of PAX6 (left) and P75 (right) from (Rakic et al. 2009). The error bar plot (bottom) shows higher expression of Pax6 in the anterior cluster and higher expression of P75 in the posterior cluster in the Lifespan database.
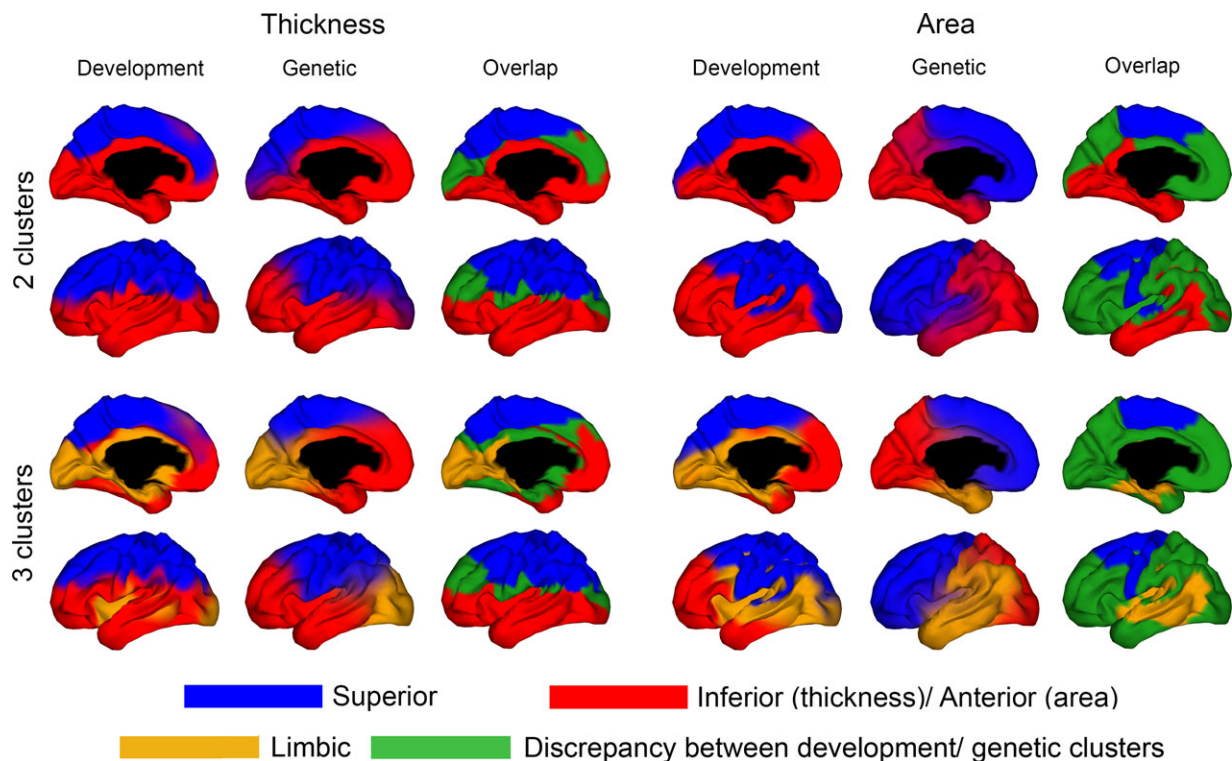

Figure 4. Comparison of developmental and genetic clusters. Thickness clusters in the left panel, area clusters in the right panel. first column is the development clusters (left hemisphere only shown), middle column is the genetic clusters from (Chen et al. 2013), right column is a conjunction map of the concordance/discrepancy of development versus genetics. Vertices belonging to the same cluster across the developmental and the genetic clusters are shown in blue/red/yellow. Vertices that are discordant between the developmental and the genetic clusters are shown in green. Thus, the size of the green area represents the amount of discrepancy between the developmental and the genetic cluster solutions. As can be seen, the overlap is better for the 2-cluster solution compared with the 3-cluster solution, and better for thickness than area.

Comparing the developmental and the genetic CT clusters, the same IS division was seen for the 2-cluster solution ($r = 0.96$ for genetics vs. 0.93 for development, RI = 0.69, adj RI = 0.39). The genetic clusters also followed the AP ($r = 0.90$) and to a lesser extent the LM ($r = 0.25$) gradient. For the 3-cluster solution, the medial delineation of the limbic developmental cluster included the medial temporal lobe and the cingulum as well as the occipital cortex, while the genetic homolog cluster did not include the occipital lobe but more of the prefrontal cortex laterally and medially. RI indicated similar genetic-developmental overlap (RI = 0.68) for the 3-cluster solutions, but adj RI dropped to 0.31, with a further drop to the 4-cluster solution (RI = 0.70, adj RI = 0.23). Thus, the overlap between CT development and genetic topography dropped with higher number of clusters.

Life Span Trajectories of Developmental Clusters

Mean CT and SA values in each cluster from the 3-cluster solutions were extracted for each participant and timepoint in the full MRI sample from 4.1 to 88.5 years, yielding 1633 observations. GAMMs with cluster as a dependent variable, age as a predictor, and a random effect for intercept showed that all

Figure 5. Random clusters. The random clusters generated using the k-means algorithm.

clusters showed highly nonlinear relationships to age (all P's < $2e^{-16}$, edf for all > 5). SA differed as a function of sex (Amlien et al. 2016) and was included as a nuisance covariate in the SA analyses. As expected, CT clusters showed mainly monotonous negative relationships to age (Fig. 2), with steeper reductions in childhood and adolescence, while SA increased in the first part of the age span (Fig. 1), peaking in early teenage years, followed by reductions for the rest of the life span.

To test whether the clusters showed unique age trajectories, analyses were repeated with all clusters for each modality (SA, CT) as simultaneous predictors of age. For SA, this yielded highly significant residual age relationships for all clusters (all P's $\leq 4.07^{-5}$). The limbic cluster showed residual reductions with higher age throughout the whole age span, while the anterior cluster showed slight increases and the posterior a U-shaped trajectory (Fig. 1, right panel, bottom). The analyses were also rerun without the cluster-forming development sample, and all clusters were still highly significantly related to age when run separately (all P's < $2e^{-16}$) and simultaneously ($n = 502, 860$ observations, all P's < 0.05), both for CT and SA.

Random Clusters

To test whether the independent life span trajectories of the developmental clusters reflected an inherent feature of any cortical cluster of a given size, we created random clusters of approximately the same size and repeated the GAMMs with all clusters as simultaneous predictors of age (Fig. 5). The developmental clusters performed substantially better than the random clusters on all model fit measures (CT: developmental clusters–random clusters, ΔAIC = −150.75, ΔBIC = −150.75, logLik = 75.38; SA: ΔAIC = −53.57, ΔBIC = −53.58, logLik = 26.79).

In conclusion, we were able to detect large cortical regions with unique and independent trajectories across the life span through data-driven clustering of longitudinal change in children. We proceeded to test whether the clusters were related to cognitive performance.
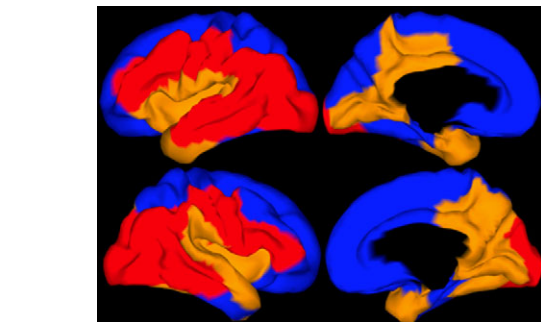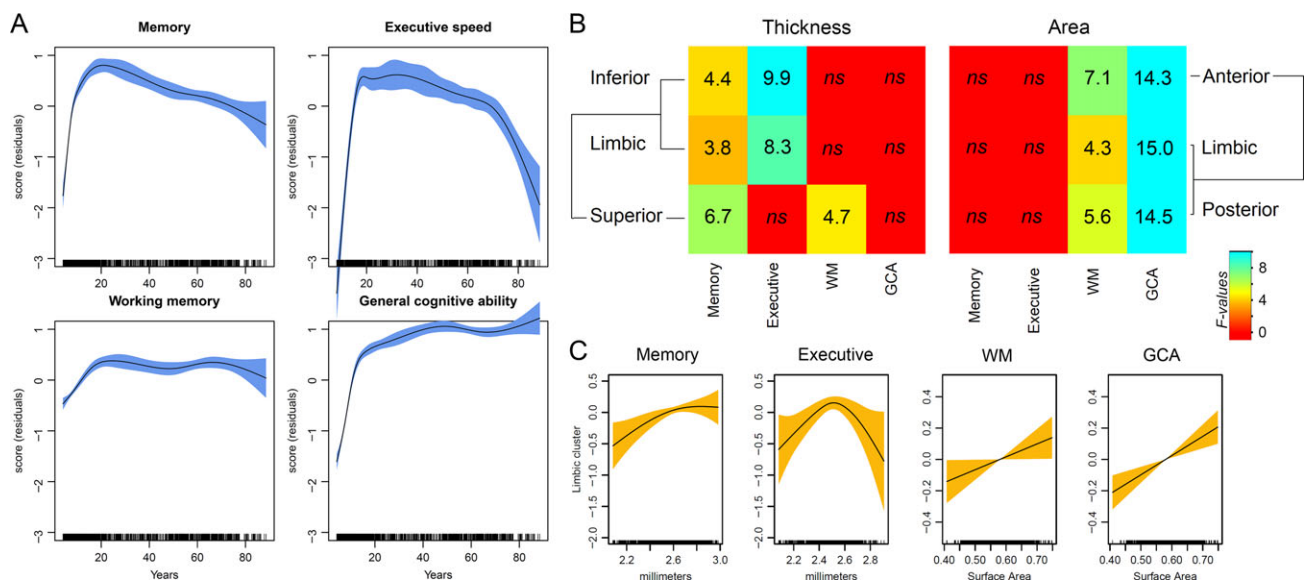

Figure 6. Cognitive relationships. (A) Each cognitive domain plotted against age, residualized on timepoint to remove retest effects. For trajectories of the tests loading highly on GCA (matrix reasoning, vocabulary) see Supplementary Material. (B) Heat maps of F-values illustrating the relationship between each cluster and each cognitive function, regressed on age and sex (SA). (C) Examples of brain cognition relationships for the limbic cluster for thickness (2 plots to the left) and area (2 plots to the right). Plots for all variables are presented in Supplementary Material. The shaded area denotes ±2 standard errors of the mean.

Cognitive Components—Relationship to Developmental Clusters

All cognitive components showed highly significant ($P < 2e^{-16}$) and nonlinear (edf ≥ 4.9) age trajectories (Fig. 6A, Table 3). Each component was then used as a dependent variable in separate GAMMs, with age and each developmental cluster as predictors, intercept as a random effect, and subject timepoint as a covariate to control for retest effects. Selected results are presented in Fig. 5C and numeric results in Tables 4 and 5 (full results in Supplementary Material). All SA clusters were positively related to GCA ($P < 0.0002$). The anterior cluster was also related to working memory span ($P = 0.008$), while the limbic ($P = 0.03$) and posterior ($P = 0.018$) did not survive Bonferroni corrections. None were related to memory or executive speed. In contrast, the CT superior cluster ($P = 0.005$) was related to memory, while the limbic and inferior (both P's = 0.02) did not survive corrections. The limbic ($P = 0.01$) and inferior ($P = 0.005$) were related to executive speed (after corrections). The relationships were nonlinear, as would be expected based on the monotone negative thickness–age relationships coupled with

the typical inverse U-shaped cognition–age relationships. The differential relationships between cognitive function and CT and SA are illustrated in the heat maps in Fig. 6B.

Discussion

The present results show that cortical expansion in childhood development follows the major gene expression patterns of factors responsible for shaping the partitioned and specialized human neocortex during prenatal development (Rakic et al. 2009). Through a data-driven parcellation of the cerebral cortex based on longitudinal change in SA in 4–12-year-old children, we were able to detect the major AP-developmental gradient known from embryonic development (Bishop et al. 2000). This demonstrates a continuity in cortical expansion from the earliest stages to the period when regional arealization reaches its peak. While this represents continuity between the fundamental principles for embryonic brain development (Rakic 1988; Rakic et al. 2009) and later childhood SA maturation, in line with known influences of neonatal characteristics on SA (Walhovd et al. 2012), CT change more strongly followed adult genetic organization principles, as predicted from previous work on genetic cortical patterning (Chen et al. 2013). Importantly, the developmental clusters showed statistically distinguishable trajectories through more than 8 decades of life, in accordance with the view that fundamental principles governing brain development in children have lasting impact on the brain. Thus, brain regions that develop together also change together through the rest of life. Finally, since SA is highly determined by prenatal factors, we expected correlations with GCA, which loads highly on the g-factor (Deary et al. 2010) and has high between-person life span stability (Lyons et al. 2009; Deary et al. 2012). This was confirmed, in contrast to CT, which was more strongly related to cognitive domains with lower loading on the g-factor (Deary et al. 2010), such as

Table 3 Effects of age on the cognitive components

	edf	F's (age)	P's (age)	R^2 (adj) model
Memory	7.36	89.5	$<2e^{-16}$	0.62
Executive speed	8.25	44.9	$<2e^{-16}$	0.77
Working memory	4.90	38.8	$<2e^{-16}$	0.36
GCA	7.01	405.5	$<2e^{-16}$	0.78

Note: GAMMs were run with age as a smooth term, subject timepoint as a linear covariate, and subject as a random effect. Adjusted R^2 refers to the full model including covariates. GCA, general cognitive ability; edf, effective degrees of freedom for the smooth term.

Table 4 Effects of cluster SA on the cognitive factors in the full sample

	edf	F	P
Memory			
Limbic	1.00	3.4	0.07
Posterior	1.00	2.8	0.09
Anterior	1.00	2.5	0.12
Executive speed			
Limbic	1.04	0.0	0.88
Posterior	1.00	0.0	0.84
Anterior	1.00	0.1	0.80
Working memory			
Limbic	1.00	4.3	**0.03**
Posterior	1.00	5.6	**0.018**
Anterior	1.00	7.1	**0.008**
GCA			
Limbic	1.00	15.0	**0.0001**
Posterior	1.00	14.3	**0.0002**
Anterior	1.00	14.5	**0.0001**

Note: GAMMs were run with age as a smooth term and cluster as a linear predictor. Subject timepoint was included as a linear covariate and subject as a random effect variable.
Bold: P < 0.05 corrected (adjusted Bonferroni correction for 4 cognitive factors and 3 clusters taking between-cluster correlations into account) **Bold italics**: P < 0.05 uncorrected.
GCA, general cognitive ability; edf, effective degrees of freedom for the smooth term (a measure of deviation from linearity).

Table 5 Effects of cortical thickness on the cognitive factors in the full sample

	edf	F	P
Memory			
s(Limbic)	2.16	3.8	0.02
s(Superior)	2.70	6.7	**0.005**
s(Inferior)	2.70	4.4	0.02
Executive speed			
s(Limbic)	3.39	8.3	**0.01**
s(Superior)	2.04	3.4	0.10
s(Inferior)	2.93	9.9	**0.005**
Working memory			
s(Limbic)	1.00	2.3	0.13
s(Superior)	1.00	4.7	**0.03**
s(Inferior)	1.00	2.2	0.14
GCA			
s(Limbic)	2.16	2.9	0.06
s(Superior)	1.00	0.0	0.98
s(Inferior)	1.00	0.0	0.90

Note: GAMMs were run with age and each cluster as smooth terms. Subject timepoint was included as a linear covariate and subject intercept as a random effect variable.
Bold: P < 0.05 corrected (adjusted Bonferroni correction for 4 cognitive factors and 3 clusters taking between-cluster correlations into account) **Bold italics**: P < 0.05 uncorrected.
GCA, general cognitive ability; edf, effective degrees of freedom for the smooth term.

Parcellation of the Developing Human Cerebral Cortex

The results showed that the cortex can be parcellated in meaningful ways based on developmental change data alone. The AP SA axis followed the major gene expression gradient identified in animal studies (Bishop et al. 2000; Rakic et al. 2009). This link was further supported in the present study through the finding of significantly different gene expression in the anterior versus the posterior cluster for PAX6 and P75, both established anterior gradient factors in embryonic development (Bishop et al. 2000). Such correspondence between childhood SA maturation and cortical ontogenesis is in line with the protomap (Rakic 1988) and radial unit tenets (Rakic et al. 2009). According to these, neural progenitors in the ventricular zone form a mosaic of proliferative units that establish an embryonic cortical map in early development. During the migration of neurons into the cortex, their position is then retained by restraints imposed through the radial glial scaffolding. However, it has not been established that these principles laid down in the first stages of CNS development are reflected in cortical maturation in later childhood in humans.

Although there was good overlap between SA and CT for the 2-cluster solution, this dropped substantially with higher cluster numbers. CT and SA are shaped by independent genes (Rakic 1988; Panizzon et al. 2009) and different neurobiological mechanisms in early fetal life (Rakic et al. 2009), and they also follow fundamentally different trajectories in development (Raznahan, Shaw, et al. 2011; Amlien et al. 2016; Walhovd et al. 2017) and aging (Storsve et al. 2014). As expected, there was a fundamental difference in the principal axis distinguishing CT and SA even for the 2-cluster solution, with the CT clusters adhering to an IS axis, with the plane of the cluster division tilted 19° for SA. While the AP SA division was seen also in a previous developmental study, the IS CT axis was not (Krongold et al. 2017). This could possibly result from methodological differences, for example, that the previous study used both combined cross-sectional and longitudinal information. A second longitudinal study with an alternative analysis approach reported indirect evidence for an IS gradient in CT development (Alexander-Bloch et al. 2013), and it has previously been suggested that such a division could be due to cytoarchitectonic features and connectivity patterns (Chen et al. 2013).

The 3- and 4-cluster solutions revealed additional interesting patterns. Not only local clusters were seen but also relationships between functionally connected regions crossing lobar boundaries. For instance, lateral prefrontal cortex and the lateral anterior temporal cortex were included in the same SA and CT clusters. This frontotemporal connection fits earlier observations (Raznahan, Lerch, et al. 2011; Krongold et al. 2017) and would be expected from structural connections represented by the uncinate fasciculus (Schmahmann and Pandya 2006). A limbic cluster encapsulating the medial temporal lobe, the cingulum and insula, and extending backward covering the lingual gyrus, cuneus, and occipital cortex was also seen for both SA and CT. This demonstrates that cortical maturation not necessarily follows lobar boundaries but rather extends beyond what would be expected from anatomical proximity. Similarly, SA of auditory cortex in the superior temporal lobe clustered together with somatosensory, motor and visual cortices in the 2-cluster solution, that is, mimicking functional clusters. Still, morphological change did not follow functional boundaries in a clear-cut manner, as calcarine sulcus (V1) and ventral visual areas clustered with the inferior/anterior cortex, not the rest of the visual cortex.

Importantly, the developmentally defined clusters showed statistically distinct life span trajectories. Although the general form of the trajectories is well known (Fjell et al. 2015; Walhovd et al. 2016), the analyses revealed residual age relationships for single clusters independently of other clusters. This finding was in accordance with the hypothesis that variations in cortical development has lifelong impacts, and consequently that regions that develop together tend to change together through the rest of life. We have previously shown that correlations between longitudinal changes in CT across predefined smaller ROIs are similar in development and aging (Fjell et al. 2015). Here, we show that the trajectories of clusters based solely on coordinated developmental change, with no anatomical restrictions imposed on the clustering, can be delineated in a sample spanning more than 80 years, both for SA and CT. Cluster solutions above 4 were not stable, which caused the clusters to be anatomically extensive. Consequently, they encompassed subregions found in previous research to show partly different developmental trajectories (Fjell et al. 2015; Amlien et al. 2016). Importantly, however, the clusters consist of regions of correlated developmental change, not necessarily regions with similar trajectories. These main regions of coordinated change will naturally generalize across subregions, but the coordination of change across the subregions was not stable enough to allow identification of coordinated change across anatomically more fine-grained regions.

Adherence to Genetic Patterning

The clusters were tested against genetic cortical patterning results (Chen et al. 2013). For CT, we found overlap between developmental and genetic patterns. This fits with our previous finding that regional differences in cortical thinning adhered to genetic organizational principles (Fjell et al. 2015). In the present study, we defined clusters based on developmental change, independently of the genetic patterning. Although the genetic overlap was lower with a higher number of clusters, certain similarities between developmental and genetic organization patterns remained, for instance, the prefrontal–temporal relationship (Chen et al. 2013). Thus, partly the same genes seem to govern absolute frontal and temporal CT. A genetic frontotemporal relationship was also seen in a developmental twin sample for CT and SA (Schmitt et al. 2017).

In contrast, there was a limited overlap between the developmental SA clusters and the genetic clusters, revealing interesting differences. Genetic SA relationships seem local or lobar, lacking strong long-distance or cross-region correlation patterns, with generally lower—and more age-invariant—correlations across the cortex (Chen et al. 2011; Schmitt et al. 2017; Strike et al. 2018). The developmental organizational patterns crossed anatomical boundaries, such as the frontotemporal and the limbic clusters. Another difference was that premotor and postcentral/somatosensory regions clustered together in development, as seen in previous fetal work (Johnson et al. 2009) but have distinct adult genetic patterns (Chen et al. 2013). Notably, the genetic-developmental similarity for CT is in line with the prediction from the original genetic patterning paper

that CT clusters would show genetic relatedness with clusters of similar maturational timing (Chen et al. 2013).

The difference in genetic overlap for CT and SA further illuminates the developmental origins hypothesis. We expected SA change to adhere to major gradients from embryonic development, and CT change to overlap with genes responsible for CT at a later point in life. SA reaches its maximum expansion in early adolescence (Amlien et al. 2016), with the major determinant likely being the number of cell division cycles of the neural stem cell pool at the premitotic stage of neural development (Rakic 2009). The width of the cortical minicolumn at birth is around one-third of its adult size (Buxhoeveden and Casanova 2002), and expansion of cortical SA in childhood can likely be explained by growth of these (Lyall et al. 2015). The developmental SA clusters likely reflect the last part of an expansion that can be traced back to embryonic stage, as also evidenced by the demonstrated adherence to the AP gradient of gene expression patterns. In contrast, CT ceases to increase early afterbirth and reaches 97% of adult values in 2 years (Lyall et al. 2015). Early CT is affected by asymmetric cell division cycles of the cortical founder pool, determining the number of cells within each column (Rakic 2009). However, the number of neurons in each column is hardly a determinant of cortical changes after the initial CT increase, which rather can be attributed to dendritic branching, synaptogenesis and gliogenesis (Huttenlocher and Dabholkar 1997). Thus, CT change from 4 to 12 years likely reflects either different processes or differences in the relative contributions of the same processes compared with CT change in very early development. Studies show that the genetic contribution to CT but not SA changes during development (Schmitt et al. 2017; Teeuw et al. 2018), and CT shows steeper slopes during adolescent development (Amlien et al. 2016) and later aging (Storsve et al. 2014) than SA. We argue that CT to a greater extent than SA reflects accumulated lifelong genetic and environmental impact. Thus, SA is usually more strongly related to early-life factors and CT relatively more also to later-life factors. Empirical support comes from studies showing larger effects of birthweight and other obstetric factors on SA than CT (Martinussen et al. 2005; Raznahan et al. 2012; Walhovd et al. 2012; Jha et al. 2018), and environmental interventions affecting CT (Engvig et al. 2010; Wenger et al. 2012).

Cognitive Correlates of Developmental Clusters

SA and CT were expected to correlate with different cognitive domains. We hypothesized that SA would be related to GCA, which shows high between-person stability across life (Lyons et al. 2009; Deary et al. 2012), likely due to the impact from early-life factors. Accordingly, we found highly significant life span relationships between GCA and the SA clusters, but not CT clusters, in line with previous observations (Vuoksimaa et al. 2015; Walhovd et al. 2016). In contrast, we speculated that since CT is more strongly related to age and sensitive to environmental influences, it would be related to more specific cognitive functions with lower loadings on the g-factor and less established lifelong between-person stability. Episodic memory and executive speed have lower g-loadings than GCA (Deary et al. 2010) and declines steeply with age (Salthouse 2004). We found relationships between these components and all CT clusters. No significant relationships were seen between executive speed and SA, while the relationships between SA and memory were just significant (limbic and posterior clusters) or showed a trend ($P = 0.06$, anterior cluster). Working memory span, which

was relatively invariant during adult life, showed comparable relationships with CT and SA. Importantly, however, greater age effects do not equal less between-person stability, and it is as of yet not clear whether memory and executive speed show less between-person stability over the life course than GCA. People differ in the amount of change in memory and speeded tasks over time (Salthouse 2016), and change in GCA is more strongly related to "global cognitive" change than changes in episodic memory and speed are (Tucker-Drob 2011). Still, correlations of change within and across cognitive domains tend to increase with age (Tucker-Drob et al. 2014), and a recent meta-analysis showed that 59% of the variance in change is shared across abilities (Tucker-Drob et al. 2018). In any case, a conclusion from the present results is that relationships between cognitive function and cortical morphometry adhere more strongly to modality than anatomical region. Vertex-wise analyses across the cortex could potentially detect more anatomically specific relationships with cognition, but at the levels of major clusters, measurement type seems more important than anatomical location.

Conclusion

In conclusion, cortical SA expansion during childhood was organized according to an AP gradient, seen also during early embryonic development, and related to gene expression and genetic patterning. Clusters of cortical development showed statistically distinct trajectories through 8 decades of life, and correlated with cognitive function in predictable ways, demonstrating continuity of human cortical development from early to late stages of life.

Supplementary Material

Supplementary material is available at *Cerebral Cortex* online.

Funding

Notes

References

Akaike H. 1974. A new look at the statistical model identification. IEEE Trans Automat Contr. 19:716–723.

Alexander-Bloch A, Raznahan A, Bullmore E, Giedd J. 2013. The convergence of maturational change and structural covariance in human cortical networks. J Neurosci. 33:2889–2899.

Amlien IK, Fjell AM, Tamnes CK, Grydeland H, Krogsrud SK, Chaplin TA, Rosa MG, Walhovd KB. 2016. Organizing principles of human cortical development—thickness and area from 4 to 30 years: insights from comparative primate neuroanatomy. Cereb Cortex. 26:257–267.

Bishop KM, Goudreau G, O'Leary DD. 2000. Regulation of area identity in the mammalian neocortex by Emx2 and Pax6. Science. 288:344–349.

Buxhoeveden DP, Casanova MF. 2002. The minicolumn hypothesis in neuroscience. Brain. 125:935–951.

Chen CH, Fiecas M, Gutierrez ED, Panizzon MS, Eyler LT, Vuoksimaa E, Thompson WK, Fennema-Notestine C, Hagler DJ Jr., Jernigan TL, et al. 2013. Genetic topography of brain morphology. Proc Natl Acad Sci USA. 110:17089–17094.

Chen CH, Gutierrez ED, Thompson W, Panizzon MS, Jernigan TL, Eyler LT, Fennema-Notestine C, Jak AJ, Neale MC, Franz CE, et al. 2012. Hierarchical genetic organization of human cortical surface area. Science. 335:1634–1636.

Chen CH, Panizzon MS, Eyler LT, Jernigan TL, Thompson W, Fennema-Notestine C, Jak AJ, Neale MC, Franz CE, Hamza S, et al. 2011. Genetic influences on cortical regionalization in the human brain. Neuron. 72:537–544.

Dale AM, Fischl B, Sereno MI. 1999. Cortical surface-based analysis. I. Segmentation and surface reconstruction. Neuroimage. 9:179–194.

Dale AM, Sereno MI. 1993. Improved localization of cortical activity by combining EEG and MEG with MRI cortical surface reconstruction: a linear approach. J Cogn Neurosci. 5:162–176.

Deary IJ, Penke L, Johnson W. 2010. The neuroscience of human intelligence differences. Nat Rev Neurosci. 11:201–211.

Deary IJ, Yang J, Davies G, Harris SE, Tenesa A, Liewald D, Luciano M, Lopez LM, Gow AJ, Corley J, et al. 2012. Genetic contributions to stability and change in intelligence from childhood to old age. Nature. 482:212–215.

Delis DC, Kramer JH, Kaplan E, Ober BA. 2000. California verbal learning test (CVLT-II). 2nd ed. San Antonio, TX: The Psychological Corporation.

Engvig A, Fjell AM, Westlye LT, Moberget T, Sundseth O, Larsen VA, Walhovd KB. 2010. Effects of memory training on cortical thickness in the elderly. Neuroimage. 52:1667–1676.

Fischl B, Dale AM. 2000. Measuring the thickness of the human cerebral cortex from magnetic resonance images. Proc Natl Acad Sci USA. 97:11050–11055.

Fjell AM, Grydeland H, Krogsrud SK, Amlien I, Rohani DA, Ferschmann L, Storsve AB, Tamnes CK, Sala-Llonch R, Due-Tonnessen P, et al. 2015. Development and aging of cortical thickness correspond to genetic organization patterns. Proc Natl Acad Sci USA. 112:15462–15467.

Fjell AM, Walhovd KB, Westlye LT, Ostby Y, Tamnes CK, Jernigan TL, Gamst A, Dale AM. 2010. When does brain aging accelerate? Dangers of quadratic fits in cross-sectional studies. Neuroimage. 50:1376–1383.

Fjell AM, Westlye LT, Amlien I, Espeseth T, Reinvang I, Raz N, Agartz I, Salat DH, Greve DN, Fischl B, et al. 2009. Minute effects of sex on the aging brain: a multisample magnetic resonance imaging study of healthy aging and Alzheimer's disease. J Neurosci. 29:8774–8783.

Glasser MF, Coalson TS, Robinson EC, Hacker CD, Harwell J, Yacoub E, Ugurbil K, Andersson J, Beckmann CF, Jenkinson M, et al. 2016. A multi-modal parcellation of human cerebral cortex. Nature. 536:171–178.

Huttenlocher PR, Dabholkar AS. 1997. Regional differences in synaptogenesis in human cerebral cortex. J Comp Neurol. 387:167–178.

Jagust WJ. 2016. Early life sets the stage for aging. Proc Natl Acad Sci USA. 113:9148–9150.

Jha SC, Xia K, Ahn M, Girault JB, Li G, Wang L, Shen D, Zou F, Zhu H, Styner M, et al. 2018. Environmental influences on infant cortical thickness and surface area. Cereb Cortex. https://doi.org/10.1093/cercor/bhy020

Johnson MB, Kawasawa YI, Mason CE, Krsnik Z, Coppola G, Bogdanovic D, Geschwind DH, Mane SM, State MW, Sestan

N. 2009. Functional and evolutionary insights into human brain development through global transcriptome analysis. Neuron. 62:494–509.

Kaufman L, Rousseeuw P. 1990. Finding groups in data: an introduction to cluster analysis. New York: Wiley.

Kremen WS, Franz CE, Lyons MJ. 2013. VETSA: the Vietnam era twin study of aging. Twin research and human genetics: the official journal of the International Society for Twin. Studies. 16:399–402.

Krongold M, Cooper C, Bray S. 2017. Modular development of cortical gray matter across childhood and adolescence. Cereb Cortex. 27:1125–1136.

Lyall AE, Shi F, Geng X, Woolson S, Li G, Wang L, Hamer RM, Shen D, Gilmore JH. 2015. Dynamic development of regional cortical thickness and surface area in early childhood. Cereb Cortex. 25:2204–2212.

Lyons MJ, York TP, Franz CE, Grant MD, Eaves LJ, Jacobson KC, Schaie KW, Panizzon MS, Boake C, Xian H, et al. 2009. Genes determine stability and the environment determines change in cognitive ability during 35 years of adulthood. Psychol Sci. 20:1146–1152.

MacLeod CM. 1992. The Stroop task: The "gold standard" of attentional measures. J Exp Psychol. 121:12–14.

Martinussen M, Fischl B, Larsson HB, Skranes J, Kulseng S, Vangberg TR, Vik T, Brubakk AM, Haraldseth O, Dale AM. 2005. Cerebral cortex thickness in 15-year-old adolescents with low birth weight measured by an automated MRI-based method. Brain. 128:2588–2596.

Miller JA, Ding SL, Sunkin SM, Smith KA, Ng L, Szafer A, Ebbert A, Riley ZL, Royall JJ, Aiona K, et al. 2014. Transcriptional landscape of the prenatal human brain. Nature. 508:199–206.

Panizzon MS, Fennema-Notestine C, Eyler LT, Jernigan TL, Prom-Wormley E, Neale M, Jacobson K, Lyons MJ, Grant MD, Franz CE, et al. 2009. Distinct genetic influences on cortical surface area and cortical thickness. Cereb Cortex. 19:2728–2735.

Rakic P. 1988. Specification of cerebral cortical areas. Science. 241:170–176.

Rakic P. 2009. Evolution of the neocortex: a perspective from developmental biology. Nat Rev Neurosci. 10:724–735.

Rakic P, Ayoub AE, Breunig JJ, Dominguez MH. 2009. Decision by division: making cortical maps. Trends Neurosci. 32:291–301.

Rand WM. 1971. Objective criteria for the evaluation of clustering methods. J Am Stat Assoc. 66:846–850.

Raznahan A, Greenstein D, Lee NR, Clasen LS, Giedd JN. 2012. Prenatal growth in humans and postnatal brain maturation into late adolescence. Proc Natl Acad Sci USA. 109:11366–11371.

Raznahan A, Lerch JP, Lee N, Greenstein D, Wallace GL, Stockman M, Clasen L, Shaw PW, Giedd JN. 2011a. Patterns of coordinated anatomical change in human cortical development: a longitudinal neuroimaging study of maturational coupling. Neuron. 72:873–884.

Raznahan A, Shaw P, Lalonde F, Stockman M, Wallace GL, Greenstein D, Clasen L, Gogtay N, Giedd JN. 2011b. How does your cortex grow? J Neurosci. 31:7174–7177.

Reuter M, Fischl B. 2011. Avoiding asymmetry-induced bias in longitudinal image processing. Neuroimage. 57:19–21.

Reuter M, Schmansky NJ, Rosas HD, Fischl B. 2012. Within-subject template estimation for unbiased longitudinal image analysis. Neuroimage. 61:1402–1418.

Reuter M, Tisdall MD, Qureshi A, Buckner RL, van der Kouwe AJ, Fischl B. 2015. Head motion during MRI acquisition reduces gray matter volume and thickness estimates. Neuroimage. 107:107–115.

Salthouse TA. 2004. Intelligence, Localizing age-related individual differences in a hierarchical structure. Intelligence. 32: 541–561.

Salthouse TA. 2016. Continuity of cognitive change across adulthood. Psychon Bull Rev. 23:932–939.

Schmahmann JD, Pandya DN. 2006. Fiber pathways of the brain. New York: Oxford University Press.

Schmitt JE, Giedd JN, Raznahan A, Neale MC. 2017. The genetic contributions to maturational coupling in the human cerebrum: a longitudinal pediatric twin imaging study. Cereb Cortex. 1–8.

Sotiras A, Toledo JB, Gur RE, Gur RC, Satterthwaite TD, Davatzikos C. 2017. Patterns of coordinated cortical remodeling during adolescence and their associations with functional specialization and evolutionary expansion. Proc Natl Acad Sci USA. 114:3527–3532.

Storsve AB, Fjell AM, Tamnes CK, Westlye LT, Overbye K, Aasland HW, Walhovd KB. 2014. Differential longitudinal changes in cortical thickness, surface area and volume across the adult life span: regions of accelerating and decelerating change. J Neurosci. 34:8488–8498.

Strike LT, Hansell NK, Couvy-Duchesne B, Thompson PM, de Zubicaray GI, McMahon KL, Wright MJ. 2018. Genetic complexity of cortical structure: differences in genetic and environmental factors influencing cortical surface area and thickness. Cereb Cortex. doi: 10.1093/cercor/bhy002. [Epub ahead of print]

Teeuw J, Brouwer RM, Koenis MMG, Swagerman SC, Boomsma DI, Hulshoff Pol HE. 2018. Genetic influences on the development of cerebral cortical thickness during childhood and adolescence in a Dutch longitudinal twin sample: the brain-scale study. Cereb Cortex. doi: 10.1093/cercor/bhy005. [Epub ahead of print]

Tucker-Drob EM. 2011. Global and domain-specific changes in cognition throughout adulthood. Dev Psychol. 47:331–343.

Tucker-Drob EM, Brandmaier AM, Lindenberger U. 2018. Coupled cognitive change in adulthood: a meta-analysis. Psychol Bull, in press.

Tucker-Drob EM, Reynolds CA, Finkel D, Pedersen NL. 2014. Shared and unique genetic and environmental influences on aging-related changes in multiple cognitive abilities. Dev Psychol. 50:152–166.

Vuoksimaa E, Panizzon MS, Chen CH, Fiecas M, Eyler LT, Fennema-Notestine C, Hagler DJ, Fischl B, Franz CE, Jak A, et al. 2015. The genetic association between neocortical volume and general cognitive ability is driven by global surface area rather than thickness. Cereb Cortex. 25: 2127–2137.

Walhovd KB, Fjell AM, Brown TT, Kuperman JM, Chung Y, Hagler DJ Jr., Roddey JC, Erhart M, McCabe C, Akshoomoff N, et al. 2012. Long-term influence of normal variation in neonatal characteristics on human brain development. Proc Natl Acad Sci USA. 109:20089–20094.

Walhovd KB, Fjell AM, Giedd JN, Dale AM, Brown TT. 2017. Through Thick and thin: a need to reconcile contradictory results on trajectories in human cortical development. Cereb Cortex. 27:1472–1481.

Walhovd KB, Krogsrud SK, Amlien IK, Bartsch H, Bjornerud A, Due-Tonnessen P, Grydeland H, Hagler DJ Jr., Haberg AK, Kremen WS, et al. 2016. Neurodevelopmental origins of lifespan changes in brain and cognition. Proc Natl Acad Sci USA. 113:9357–9362.

Walhovd KB, Tamnes CK, Bjornerud A, Due-Tonnessen P, Holland D, Dale AM, Fjell AM. 2015. Maturation of cortico-subcortical structural networks-segregation and overlap of medial temporal and fronto-striatal systems in development. Cereb Cortex. 25:1835–1841.

Wechsler D. 1999. Wechsler abbreviated scale of intelligence. San Antonio, TX: The Psychological Corporation.

Wechsler D. 2008. Wechsler adult intelligence scale. 4th ed. San Antonio, TX: Pearson Assessment.

Wenger E, Schaefer S, Noack H, Kuhn S, Martensson J, Heinze HJ, Duzel E, Backman L, Lindenberger U, Lovden M. 2012. Cortical thickness changes following spatial navigation training in adulthood and aging. Neuroimage. 59:3389–3397.

Wood SN 2006. Generalized Additive Models: An Introduction with R: Chapman and Hall/CRC.

Wood SN. 2011. Fast stable restricted maximum likelihood and marginal likelihood estimation of semiparametric generalized linear models. J R Stat Soc (B). 73:3–36.

Zielinski BA, Gennatas ED, Zhou J, Seeley WW. 2010. Network-level structural covariance in the developing brain. Proc Natl Acad Sci USA. 107:18191–18196.